

PMMA의 현탁 및 유화 공중합에 의한 아이코산의 미세캡슐화: 공단량체 및 가교제의 영향에 대한 정성적 분석

최보나* · 김정수†^{ORCID}

충남대학교 고분자공학과, *덕산 네오룩스

(2018년 11월 4일 접수, 2018년 11월 13일 수정, 2018년 11월 13일 채택)

Microencapsulation of Eicosane with Suspension and Emulsion Copolymerizations of PMMA: A Qualitative Evaluation of the Effects of Comonomers and Crosslinkers

Bona Choi* and Jeong Soo Kim†^{ORCID}

Dept. of Polym. Sci. & Eng., Chungnam National Univ., 99 Daehack-Ro, Daejeon 34134, Korea

*Duksan Neolux, Ssukgol-gil 21-32, Cheonan-Si 31027, Korea

(Received November 4, 2018; Revised November 13, 2018; Accepted November 13, 2018)

초록: 파라핀계 상변환 축열재의 응용 확대를 위해 모델 물질로 탄소수 20개인 아이코산을 택하고 이를 분산중합에 의해 미세캡슐화한 후 그 축열 거동을 관찰하였다. 메틸 메타크릴레이트(MMA)을 기본 단량체로 하고 유화중합법과 현탁중합법이 사용되었으며, 공단량체로는 메틸 메타크릴산(MAA), 에틸 메타크릴레이트(EMA), 부틸 메타크릴레이트(BMA)가 사용되었다. 미세캡슐화 방법을 달리하는 인자로는 중합법, 공단량체의 종류 및 무게분율, 가교제의 종류 및 투입량이 있다. 미세캡슐화 입자의 모폴로지, 입자 크기, 미세피낭 효율, 열적 거동 등이 관찰되었으며, 이들의 관찰은 FTIR, SEM, DSC, TGA를 통해 이루어졌다.

Abstract: Eicosane, which is a saturated linear hydrocarbon with 20 carbons, was selected as a core phase change material (PCM) for microencapsulation with dispersion polymerizations. The microencapsulation reactions were carried out by emulsion and suspension copolymerization of methyl methacrylate (MMA) with comonomers such as methacrylic acid (MAA), ethyl methacrylate (EMA), and butyl methacrylate (BMA). The preparation methods were diversified through varying different factors, such as polymerization method, the kinds and composition of comonomers, and crosslinking agents. The morphology, particle sizes, and thermal properties including encapsulation efficiency of the prepared microcapsules were analyzed using Fourier transform infrared spectroscopy, scanning electron microscopy, differential scanning calorimetry, and thermogravimetric analysis.

Keywords: microencapsulation, phase change material, eicosane, copolymerization, crosslinking, morphology.

Introduction

Energy supply is getting worse with rapid economic and industrial development and expansion throughout the whole world. Since the energy crisis in 1970s, the researches on renewable and sustainable energy have been attracting more attention. The storage technologies of energy using phase change materials (PCMs), which realize the storage, trans-

portation, and utilization of thermal energy, solve the problem of supply-demand mismatch in time and space, enhance energy utilization, and relieve energy crises. Therefore, phase change energy storage technology can be applied to many fields, such as solar energy storage, waste heat recovery, building heating and cooling systems, battery thermal management systems, and so on.¹

PCMs are applicable usually as thermal energy storage due to their available latent heat. Paraffin waxes are known as the most attractive PCMs due to their cost, chemical inertness, and relatively higher latent heat, which show no super-cooling or phase separation in comparison with inorganic salt hydrates.

†To whom correspondence should be addressed.
jskim@cnu.ac.kr, ORCID[®]0000-0003-2055-4847
©2019 The Polymer Society of Korea. All rights reserved.

Their practical usage is, however, limited due to the low thermal conductivity and the ecological contamination resulting from leakage during the phase change. Eicosane, which is a linear saturated hydrocarbon with 20 carbons, was selected as a core material due to its melting point adjusting to the thermal energy management in usual house-life.

The protection of paraffin PCMs through their microencapsulation with polymer usually not only enhances the thermal conductivity, but also blocks the leakage of core PCMs.^{1,2} The selection of polymeric shell material used in the microencapsulation of PCMs plays the most important role in controlling and adjusting the frame structure, mechanical strength, and thermal stability. The frequently used polymeric systems are polyurea,³⁻⁷ melamine-formaldehyde,⁸ silica,⁹ polystyrene,^{10,11} poly(methyl methacrylate) (PMMA).¹² Among them, PMMA, which is a representative materials of acrylic resins, is the most frequently used polymeric system, which is assumed to be due to its low toxicity, chemical stability, and relatively higher toughness.¹³

Although studies on the microencapsulation of PCMs using PMMA as a shell material have been reported by several groups, it is very difficult to find studies concerning the effect of comonomers on the characteristics of the microencapsulation. In this study, four acrylic comonomers were used for the formation of the shell in the microencapsulation of eicosane, with their chemical structures shown in Figure 1. Methacrylic acid (MAA) was chosen to give the shell hydrophilic property with its carboxylic group and hardness, which is assumed to result from the glass transition temperature of 228 °C. On the

other hand, ethyl methacrylate (EMA) and butyl methacrylate (BMA) were selected to give the shell hydrophobic property with their alkyl group and softness that are expected due to the glass transition temperatures of 66 °C and 15 °C, respectively.

Additionally, three kinds of crosslinkers – divinyl benzene (DVB), allyl methacrylate (AMA), and ethylene glycol dimethacrylate (EGDMA) – were chosen as other variants for the microencapsulation of paraffin PCM through dispersion polymerization. The variations in PCM core material were not considered to remove complexity, which is fixed to the compound eicosane (C₂₀H₄₂, m.p.: 36 °C).

The surface morphology, thermal stability, and the storage behavior of thermal energy were qualitatively investigated with varying amounts of comonomers and crosslinking agents.

Experimental

Materials. Eicosane, DVB, ferrous sulphate (FeSO₄·7H₂O), 70% *tert*-butyl hydroperoxide solution, and poly(vinyl pyrrolidone) (PVP) were purchased from Sigma Aldrich. Ammonium persulphate (APS), MMA, EMA, and BMA were supplied by Junsei. MAA and AMA were obtained from TCL. EGDMA was purchased from Polysciences. Benzoyl peroxide, sodium thiosulphate (Na₂S₂O₇), and methanol were supplied by Samchun Chemical Co. Ltd., Korea. The MMA monomer was purified by washing in NaOH aqueous solution (10 wt/v%). The other chemicals were used without further purification.

Preparation of Microcapsules. Suspension Polymerization: The microencapsulation reaction was carried out in a 500-mL three-neck round-bottomed flask equipped with water thermostat bath, mechanical stirrer, and a nitrogen gas inlet tube. The reaction medium was composed of two phases: a continuous phase containing 100 mL of deionized water and 1 g PVP and a discontinuous phase containing 9 g acrylic-based monomers, 12 g eicosane, 0.3 g BPO, and 3 g crosslinking agent. The continuous phase was transferred into the reaction flask with mild agitation. The initiator was premixed with monomers, PCM, and crosslinking agent. Next, the discontinuous phase was added into the continuous phase under constant stirring rate of 400 rpm following the maintenance of temperature of 75 °C for 5 h. The resultant microcapsules were filtered and repeatedly washed with methanol to remove impurities and unencapsulated paraffin wax. The purified microcapsules were then dried at room temperature. Table 1 shows the recipes used in the preparation of all samples by suspension

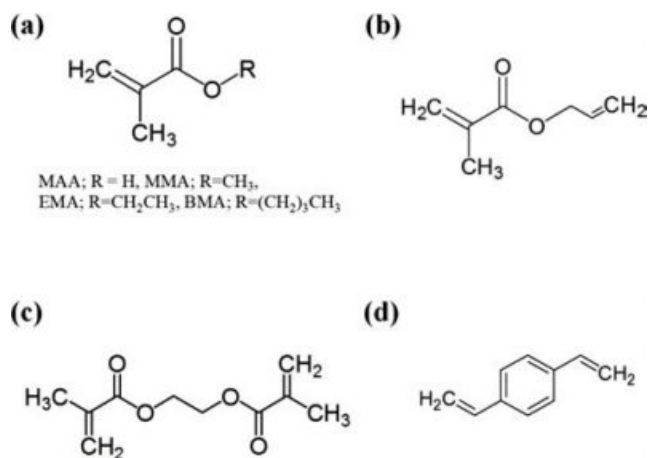


Figure 1. Chemical structures of acrylic monomers and crosslinking agents used in this study: (a) MAA; MMA; EMA; BMA; (b) AMA; (c) EGDMA; (d) DVB.

Table 1. Preparation of Microcapsules by Suspension Polymerization

Sample code ^a	MMA (g)	Comonomer (g)	Crosslinking agent (g)	Eicosane (g)
SN-NON	9	-	-	12
SA-NON	9	-	3	12
SE-NON	9	-	3	12
SD-NON	9	-	3	12
SE-MAA10	8.1	0.9	3	12
SE-MAA20	7.2	1.8	3	12
SE-MAA30	6.3	2.7	3	12
SE-EMA10	8.1	0.9	3	12
SE-EMA20	7.2	1.8	3	12
SE-EMA30	6.3	2.7	3	12
SE-BMA10	8.1	0.9	3	12
SE-BMA20	7.2	1.8	3	12
SE-BMA30	6.3	2.7	3	12

^aThe microcapsule sample codes were used as follows: The first letter before dash denotes polymerization method (S, suspension; E, emulsion) and second denotes the initial of crosslinking agents (N, no crosslinker; A, allyl methacrylate; E, ethylene glycol dimethacrylate; D, divinyl benzene). The following three letters after the dash are abbreviations of acrylic comonomer, including NON (no comonomer). The last two digits denote the weight portion of the comonomer in the monomer mixture.

polymerization.

Emulsion Polymerization: The apparatus and equipment were the same as described in the previous suspension polymerization. The continuous phase containing 99 mL deionized water and 2 g Triton X-100 as a surfactant were transferred into the reaction flask at 40 °C with a stirring rate of 500 rpm. Acrylic monomers with total weight 23.5, 2.5 g crosslinking agent, and 25 g eicosane were assembled in oil phase. Then, oil phase was added into the reaction flask with a stirring rate of 900 rpm for 10 min before polymerization. Then, 0.25 g of APS and 1 mL freshly prepared FeSO₄·7H₂O solution (prepared by mixing 0.3 g of FeSO₄·7H₂O with 200 mL water) were added and stirred for 30 min. An extra 0.25 g Na₂S₂O₇ and 1 g 70% *tert*-butyl hydroperoxide solution were added as secondary initiator and heated to 80 °C, maintained with a stirring rate of 500 rpm for 4 h. Addition of a secondary initiator during polymerization can produce uniformly sized and shaped microcapsules with high yield without a separate subsequent process. The resultant microcapsules were filtered and washed with deionized water sufficiently to remove impurities and uncapsulated paraffin wax. The obtained powders were dried

Table 2. Preparation of Microcapsules by Emulsion Polymerization

Sample code ^a	MMA (g)	Comonomer (g)	Crosslinking agent (g)	Eicosane (g)
EN-NON	23.5	-	-	25
EA-NON	23.5	-	2.5	25
EE-NON	23.5	-	2.5	25
ED-NON	23.5	-	2.5	25
EE-MAA10	21.15	2.35	2.5	25
EE-MAA20	18.8	4.7	2.5	25
EE-MAA30	16.45	7.05	2.5	25
EE-EMA10	21.15	2.35	2.5	25
EE-EMA20	18.8	4.7	2.5	25
EE-EMA30	16.45	7.05	2.5	25
EE-BMA10	21.15	2.35	2.5	25
EE-BMA20	18.8	4.7	2.5	25
EE-BMA30	16.45	7.05	2.5	25

^aThe sample codes are the same described in Table 1.

in a vacuum oven at 30 °C for 1 day. The recipe conditions used for the preparation of all samples by emulsion polymerization are summarized in Table 2.

Characterization. Fourier transform infrared (FTIR) spectra of microcapsules were obtained using an ALPHA-P ATR from Bruker. The morphologies of encapsulated particles were observed with JSM-700F SEM from Jeol. The thermal behavior of microcapsules was investigated with samples of around 5 mg under the nitrogen atmosphere at a heating rate of 5 °C/min with a differential scanning calorimeter (DSC-4000) of Perkin Elmer. In addition, phase-change behavior of microcapsules containing eicosane should be analyzed with two parameters – i.e. encapsulation ratio (*R*) and encapsulation efficiency (*E*) –, which can be calculated by the DSC results.¹³ The *R* and *E* values are determined according to eq. (1) and eq. (2), respectively,

$$R = \frac{\Delta H_{m, \text{Microcapsules}}}{\Delta H_{m, \text{PCM}}} \times 100\% \quad (1)$$

$$E = \frac{\Delta H_{m, \text{Microcapsules}} + \Delta H_{c, \text{Microcapsules}}}{\Delta H_{m, \text{PCM}} + \Delta H_{c, \text{PCM}}} \times 100\% \quad (2)$$

where $\Delta H_{m, \text{PCM}}$ and $\Delta H_{c, \text{PCM}}$ are the melting and crystallization enthalpies of pure eicosane, respectively. $\Delta H_{m, \text{Microcapsules}}$ and $\Delta H_{c, \text{Microcapsules}}$ are the melting and crystallization enthalpies of eicosane in microcapsules, respectively.

The TGA thermogram was obtained with a TGA from Mettler-Toledo; it was scanned from 30 to 600 °C with a heating rate of 10 °C/min under a nitrogen atmosphere.

Results and Discussion

FTIR Spectra. Figures 2 and 3 show the FTIR spectra of pure eicosane and selected microcapsules prepared with varying crosslinking agent and 10% acrylic comonomers by suspension and emulsion polymerization, respectively. First, the intense peaks at 2925 and 2830 cm^{-1} in pure eicosane represent the C–H stretching vibration. All microcapsules prepared by suspension polymerization show the same peaks, in which C–H stretching vibration of eicosane and polymer shell might be

assigned to be overlapped. The C–H stretching peaks of eicosane are usually strong irrespective of particle diameters which might cause total reflection only on the shell thicker than 2 μm . In the process of specimen preparation of FTIR-ATR, the microcapsules were assumed to be broken and lead the leakage of eicosane. The peaks at around 1469, 1387 and 715 cm^{-1} , which can be observed in both pure eicosane spectrum and each microcapsule spectrum, are the characteristic bands for eicosane. Spectra of all microcapsules have peaks at about 1727 and 1145 cm^{-1} , which is attributed to C=O stretching vibration and C–O stretching of the ester group in the polymer shell, respectively. The weak peak at 1660 cm^{-1} observed in the spectra of microcapsule with DVB (SD-NON, ED-NON) as crosslinking agent can be assigned to the benzene

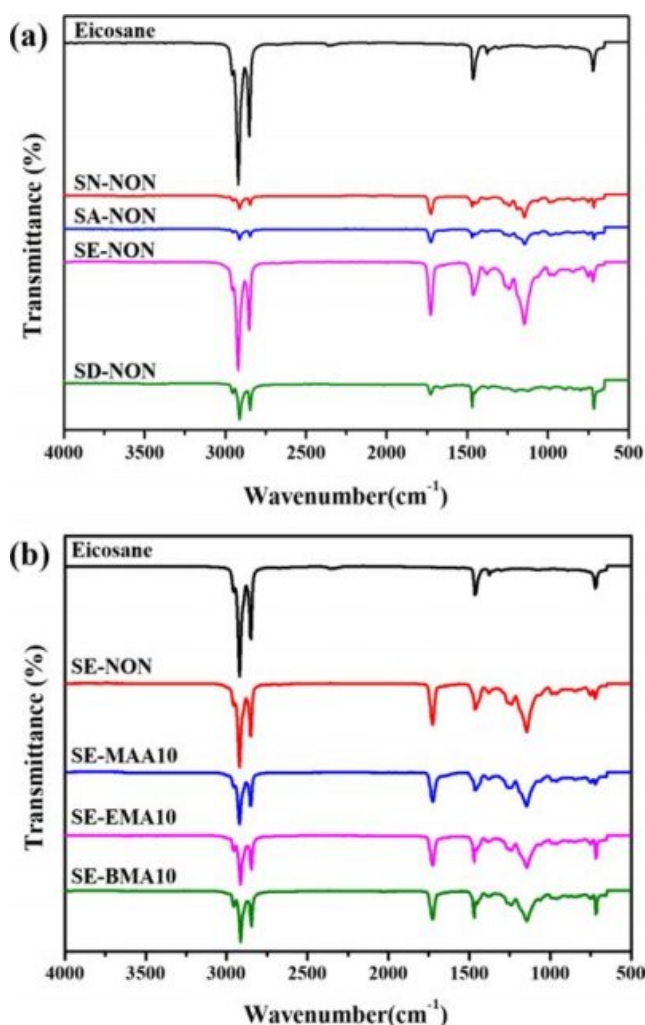


Figure 2. FTIR spectra of the microcapsules prepared by suspension polymerization with different crosslinking agents (a); different acrylic comonomers (b).

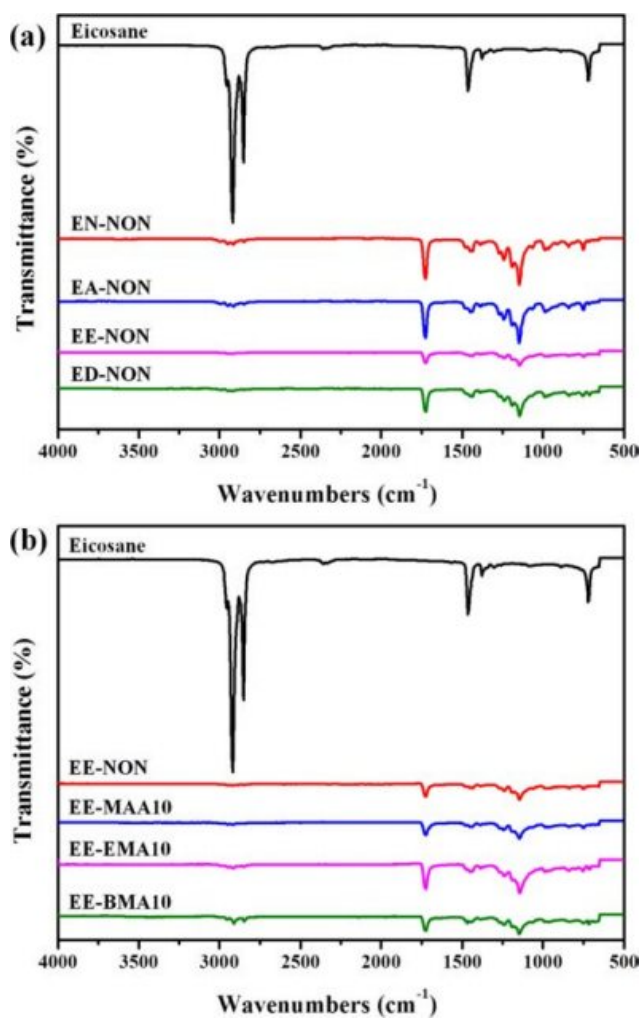


Figure 3. FTIR spectra of the microcapsules prepared by emulsion polymerization with different crosslinking agents (a); different acrylic comonomers (b).

ring stretching vibration. Thus, it can be concluded that FTIR spectra of all microcapsules have the characteristic peaks of both polymer shells and eicosane, which verifies the success for microencapsulation of eicosane as a core. In the case of emulsion polymerization, the relative intensities of C–H stretching to C=O stretching are almost very weak in comparison with suspension polymerization, which means that the weight portions of encapsulated eicosane are small.

Surface Morphology of Microcapsules. The shape and surface morphology of prepared microcapsules were observed through SEM. The microcapsules prepared by suspension polymerization with various crosslinking agent are shown in Figure 4. The surfaces of microcapsules are usually very uneven, which is assumed to be due to the difference of density between monomers and polymers. The explanation for the uneven surface of microcapsules is that it is formed from vol-

ume shrinkage of liquid eicosane in the transformation to solid.¹³ Additionally, the shape of microcapsules frequently shows a pomegranate structure composed of many smaller (approx. 1 μm) particles.¹² Regardless, a thinner shell is assumed to be formed because the ratio of polymeric shell to core of eicosane is always 1.

Figure 4 shows the SEM images of microcapsules, which differ only in crosslinking agent used. The microcapsules prepared without using crosslinking agent seemed to be broken in the shell, which means that the presence of crosslinking agent is essential in the polymerization reaction of the encapsulation process. However, in the microcapsules prepared with input of crosslinking agents as shown at Figure 4(b), (c), and (d), their spherical shapes are fairly well retained, which enhances the possibility of including eicosane in the core. Especially, the microcapsules prepared with the input of DVB show relatively bigger and smoother sinks at the surface of shell, resulting from the hard chain network of shell polymers because DVB has aromatic moiety in chemical structure in comparison with wholly aliphatic AMA and EGDMA.¹³

Figures 5, 6, and 7 show the SEM images of microcapsules different only in used comonomers in suspension polymer-

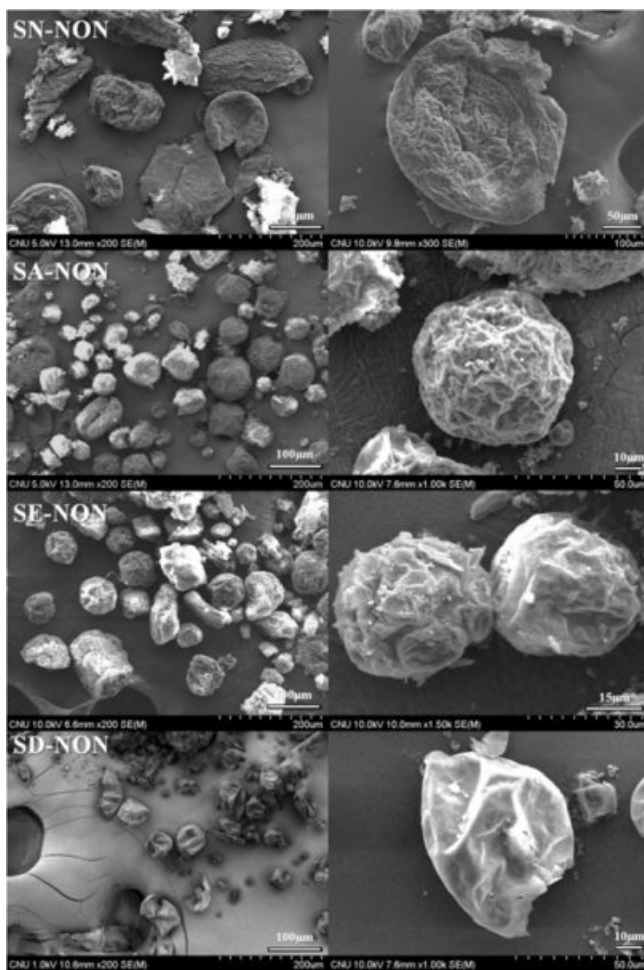


Figure 4. SEM images of the microcapsules prepared by suspension polymerization with various crosslinkers.

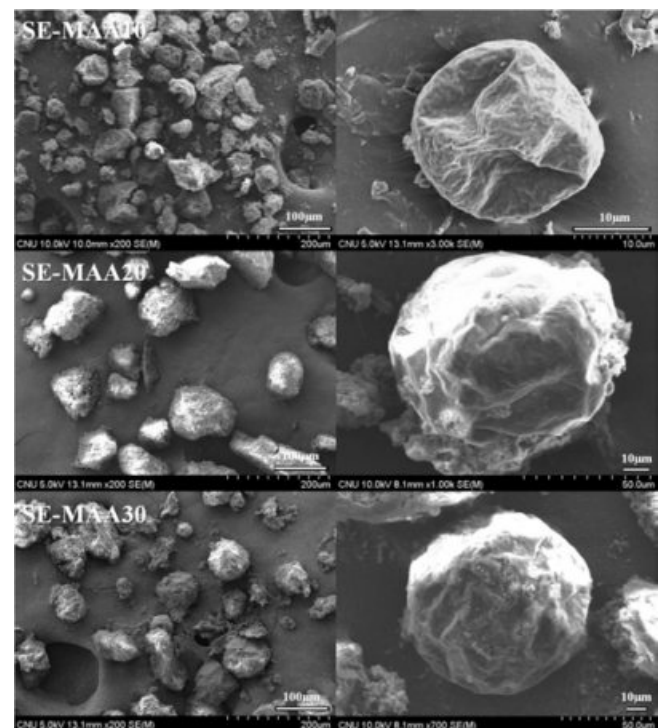


Figure 5. SEM images of the microcapsules prepared with the input of different weight portion of comonomer MAA through suspension polymerization.

ization. The reported glass transition temperatures of homopolymers of PMMA, PMAA, PEMA, and PBMA are 120, 228, 65, and 20 °C, respectively, which affects the hardness of the polymerized shell part of microcapsules.

The microcapsules prepared with MAA as comonomers have relatively smoother surface, as shown in Figure 5, which is due to the higher hydrophilicity of MAA and hardness of copolymers. Figures 6 and 7 show the surface morphology of microcapsules prepared by using comonomer EMA and BMA, respectively. In both cases, many microparticles are observed that do not contain eicosane PCM. These microparticles are assumed to be formed from the phase separation in the shell formation process, the cause of which is the increased hydrophobicity of copolymer with input of EMA and BMA. In the case of using BMA as comonomer, relatively many more wrinkles are observed at the surfaces of microcapsules, as shown in Figure 7, which are caused by the softness of copolymer shell that is less resistant to the density change due to the polymerization process.

The microcapsules obtained by emulsion polymerization show degree of surface morphology difference from ones of suspension polymerization. They are usually much smaller in

particle size, spread under 20 μm , and have a much smoother surface. Additionally, they are obtained in the cluster form of particles, which are almost formed in the drying process.¹⁴ Figure 8 shows that the effect of crosslinking agent on the particles and their surface morphology is very critical in the case of emulsion polymerization. The uneven surface of emulsion particle, which is usually not observed in conventional emulsion polymerization, is always observed in these microcapsules, which are also resulted from the large density change of polymer shell as well as eicosane PCM core. In the absence of crosslinking agent, as shown in Figure 8(a), the microcapsules show the highest roughness. The microcapsules prepared using AMA show relatively smoother surface, with the particle diameter of 200-300 nm that is estimated as a size-range of usual emulsion polymerization. On the other hand, the apparent shape of microcapsules prepared with EGDMA as crosslinking agent is very irregular and diverse, the cause of which will be analyzed more precisely in future. The microcapsules prepared with DVB as crosslinker are spheres having rough surface and narrow size distribution. The latter two cases of EGDMA and DVB show much larger particle size than conventional emulsion polymerization.

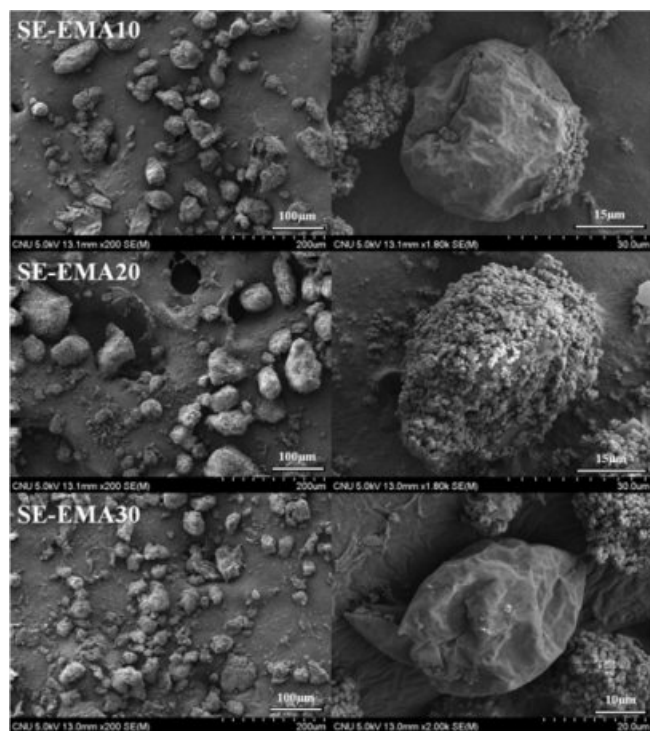


Figure 6. SEM images of the microcapsules prepared with the input of different weight portion of comonomer EMA through suspension polymerization.

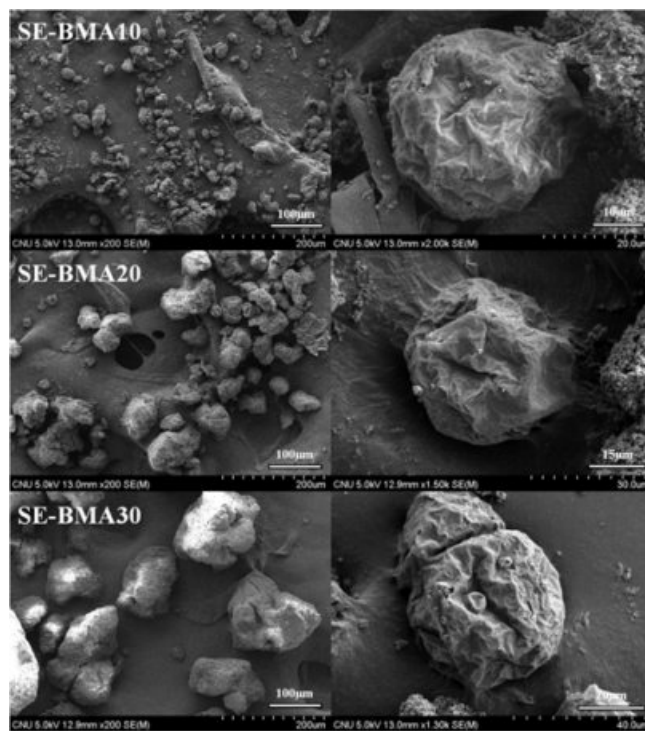


Figure 7. SEM images of the microcapsules prepared with the input of different weight portion of comonomer BMA through suspension polymerization.

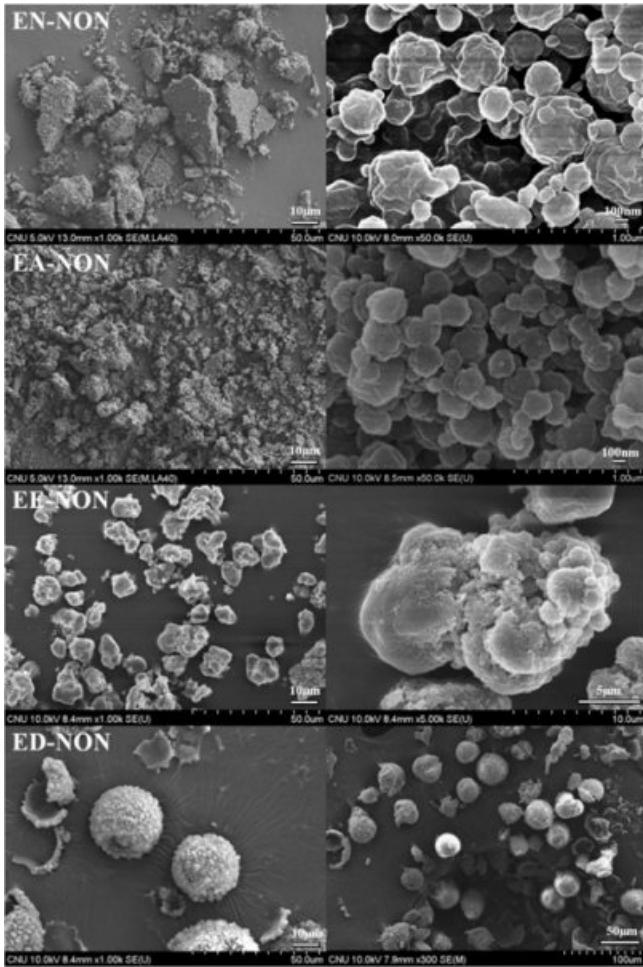


Figure 8. SEM images of the microcapsules prepared by emulsion polymerization with various crosslinkers.

Figures 9, 10, and 11 show the microcapsules prepared by replacing comonomer with MAA, EMA, and BMA, respectively, and additionally by changing their quantity of input. By using MAA as a comonomer in microencapsulating polymerization reaction, rough spherical microparticles having diameters of 200-300 nm were obtained. Their diameters are observed to increase usually in proportion to the quantity of MAA, and the hydrophilicity of MAA is assumed as an important factor to form these spherical microparticles.¹² In the case of using more hydrophobic and softer comonomers EMA and BMA, bigger and clustered microparticles were observed. Such phenomena are more clearly observed in the case of using the softer comonomer of BMA.

Phase-changing Thermal Behaviors of Microcapsules. The latent heat properties and phase transition temperatures of microcapsules were analyzed through DSC. Figures 12 and 13

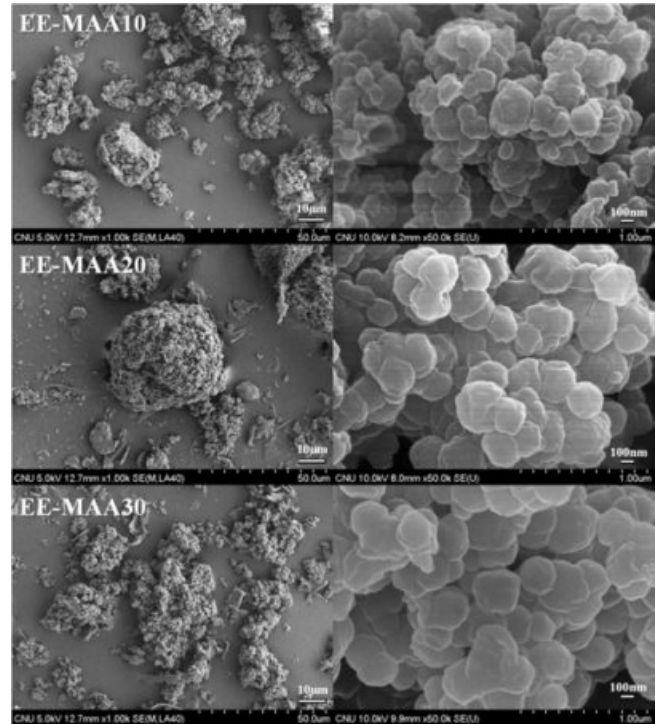


Figure 9. SEM images of the microcapsules prepared with various weight portions of comonomer MAA through emulsion polymerization.

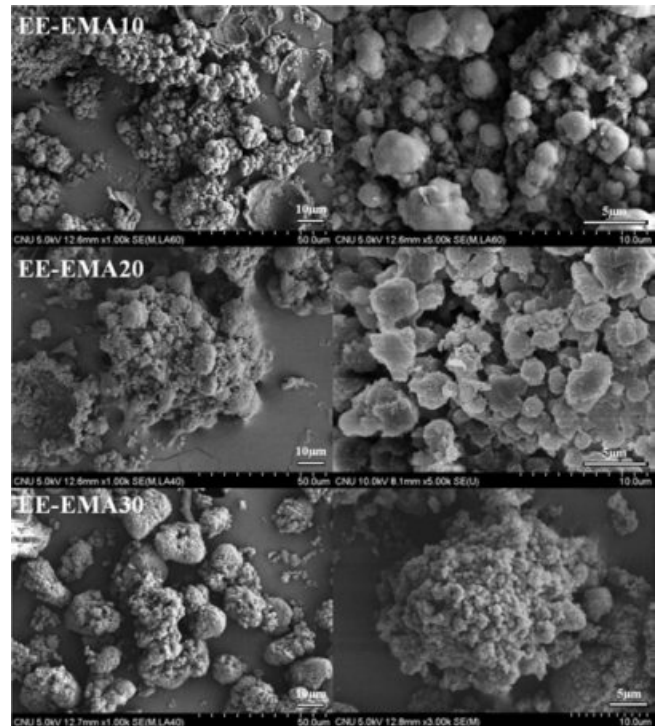


Figure 10. SEM images of the microcapsules prepared with various weight portions of comonomer EMA through emulsion polymerization.

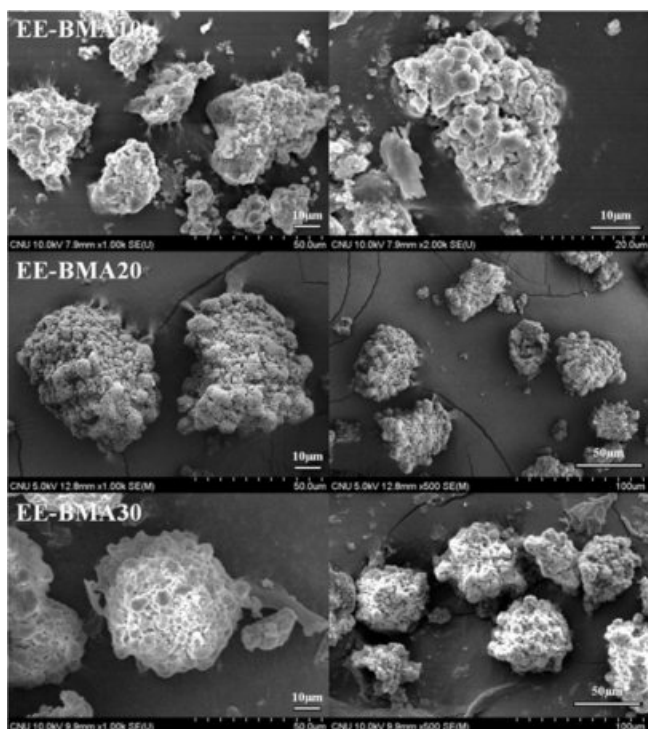


Figure 11. SEM images of the microcapsules prepared with various weight portions of comonomer BMA through emulsion polymerization.

show thermal behaviors of microcapsules that are different in crosslinking agent and comonomers in microencapsulating reaction with suspension polymerization, respectively. On the other hand, Figures 14 and 15 show the same thermal behavior in the case of using emulsion polymerization methods.

The melting transition of solid eicosane into liquid results in

an endothermic peak in the DSC diagram, while its freezing into crystal results in an exothermic peak. The exothermic peak of crystallization splits into two peaks, which correspond to two crystallization temperatures of α - and β -crystal phase, respectively. The smaller α -peak of lower temperature is reported to be due to the heterogeneous crystallization of eicosane nucleated with another chemicals while the larger β -peak is caused by homogeneous crystallization nucleated by eicosane itself. In pure eicosane, a sharp α -peak is also observed, which is nucleated by the impurity in eicosane.^{3,15}

All the thermal characteristics of microcapsules prepared through suspension and emulsion polymerization are summarized on the Tables 3 and 4, respectively. The microcapsules prepared by using suspension polymerization always have much higher encapsulation efficiencies than the microcapsules using emulsion polymerization. Figures 12-15 show the comparative DSC thermograms of microcapsules prepared in this study.

Irrespective of polymerization methods for the encapsulation of eicosane, the encapsulation efficiencies decrease critically if no crosslinker is added, which causes a large decrease of latent heat. Among the microcapsules prepared using crosslinkers, the microcapsules containing DVB moieties show the highest encapsulation efficiency, which denotes that the compact and hydrophobic crosslinkers are more effective for the encapsulation of paraffin PCM.

The effect of inputting comonomers on the latent heat of microcapsules was also qualitatively analyzed. In both polymerization methods, the use of MAA as crosslinking agent is thought to be not proper for the encapsulation of paraffins,

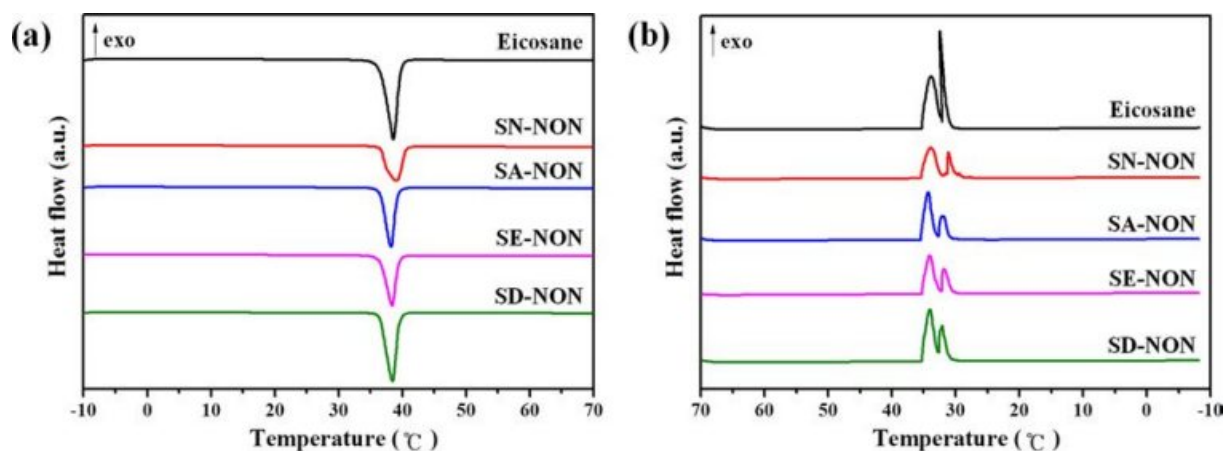


Figure 12. DSC heating (a); cooling (b) thermograms of microcapsules prepared by suspension polymerization using various crosslinking agents.

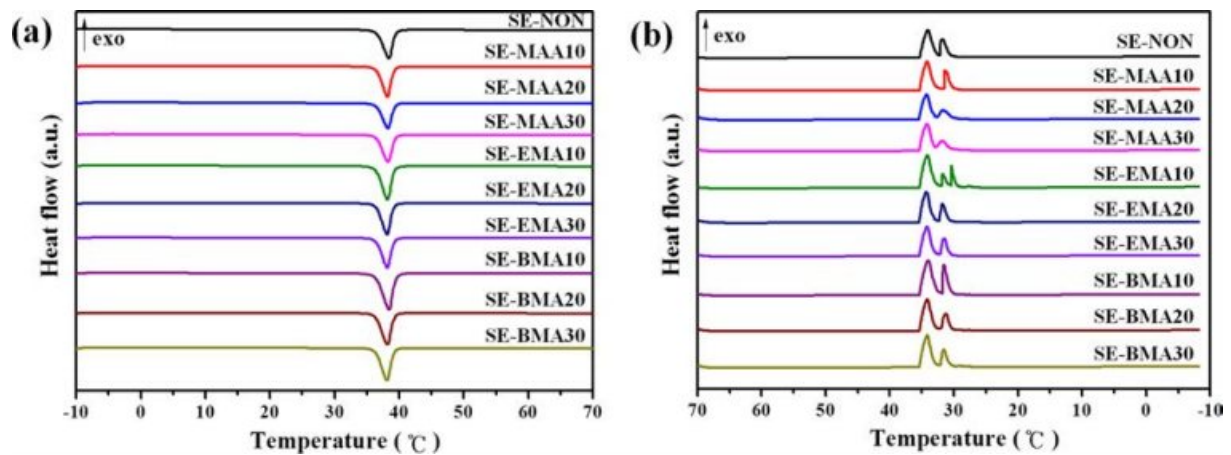


Figure 13. DSC heating (a); cooling (b) thermograms of microcapsules prepared by suspension polymerization using various comonomers different in their weight portions.

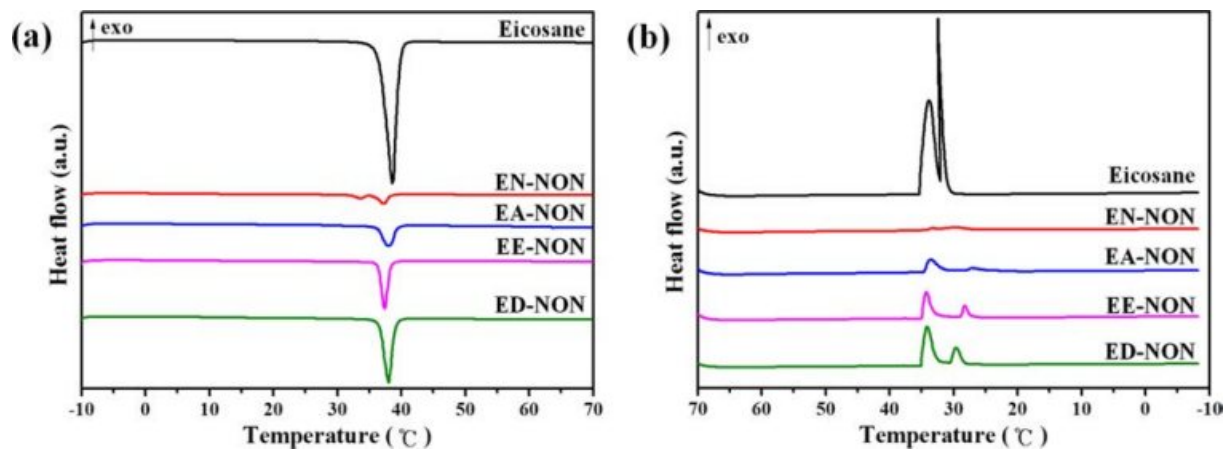


Figure 14. DSC heating (a); cooling (b) thermograms of microcapsules prepared by emulsion polymerization using various crosslinking agents.

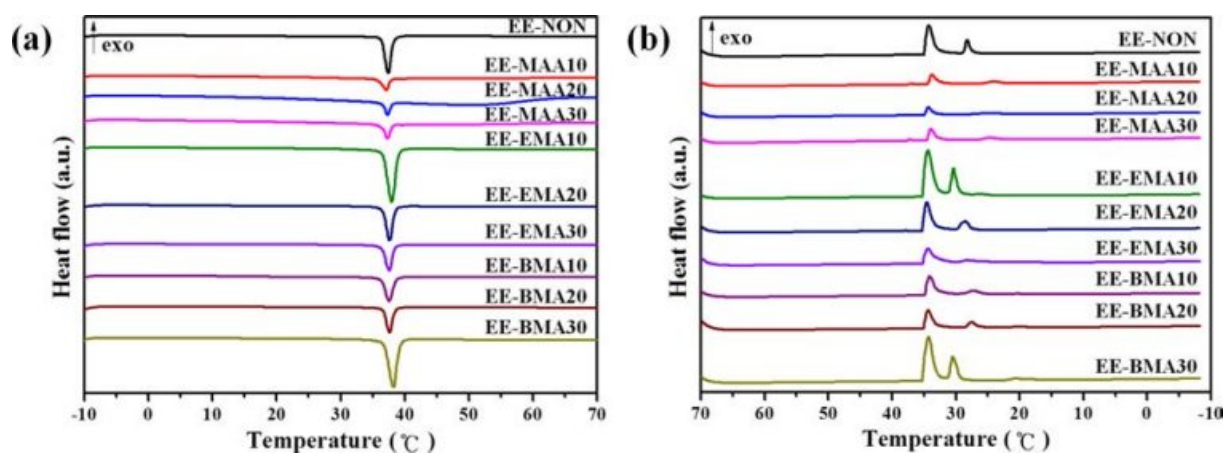


Figure 15. DSC heating (a); cooling (b) thermograms of microcapsules prepared by emulsion polymerization using various comonomers with various compositions.

Table 3. Thermal Characteristics of Microcapsules Prepared by Suspension Polymerization

Sample	ΔH_m (J/g)	ΔH_c (J/g)	T_m (°C)	T_c (°C)	R (%)	E (%)
Eicosane	257.15	250.32	38.59	32.48	-	-
SN-NON	165.49	164.67	39.12	33.88	65.06	64.36
SA-NON	160.84	158.01	38.22	34.32	62.83	62.55
SE-NON	177.77	173.97	38.43	34.11	69.31	69.13
SD-NON	209.25	204.76	38.50	34.02	81.58	81.37
SE-MAA10	156.35	152.71	38.17	34.19	60.90	60.80
SE-MAA20	153.82	150.63	38.31	34.23	60.40	59.82
SE-MAA30	143.21	135.48	38.29	34.27	54.92	55.69
SE-EMA10	171.96	168.33	38.21	34.15	67.06	66.87
SE-EMA20	159.36	156.21	38.17	34.38	62.18	61.97
SE-EMA30	157.14	154.62	38.18	34.20	61.43	61.11
SE-BMA10	188.30	183.42	38.44	34.09	73.25	73.23
SE-BMA20	154.48	151.00	38.24	34.14	60.20	60.07
SE-BMA30	158.60	155.09	38.15	34.22	61.81	61.68

Table 4. Thermal Characteristics of Microcapsules Prepared by Emulsion Polymerization

Sample	ΔH_m (J/g)	ΔH_c (J/g)	T_m (°C)	T_c (°C)	R (%)	E (%)
Eicosane	257.15	250.32	38.59	32.48	-	-
EN-NON	23.54	24.59	37.22	29.53	9.48	9.15
EA-NON	51.97	53.32	38.02	33.56	20.75	20.21
EE-NON	58.80	53.81	37.42	34.28	22.19	22.87
ED-NON	83.44	78.43	38.03	34.17	31.90	32.45
EE-MAA10	16.65	15.67	37.11	33.80	6.37	6.47
EE-MAA20	14.47	14.74	37.25	34.45	5.76	5.63
EE-MAA30	22.58	20.82	37.26	33.97	8.55	8.78
EE-EMA10	89.77	87.62	37.93	34.42	34.96	34.91
EE-EMA20	65.55	62.20	37.60	34.60	25.17	25.49
EE-EMA30	46.94	45.50	37.57	34.31	18.21	18.25
EE-BMA10	41.57	38.02	37.57	34.08	15.68	16.17
EE-BMA20	43.82	42.32	37.65	34.31	16.97	17.04
EE-BMA30	92.88	88.52	38.20	34.32	35.64	36.12

which is due to the large decrease of encapsulation efficiencies. In comparison with MAA, EMA and BMA are much better in using them as comonomers, which result in higher values of encapsulation efficiencies. Additionally, regardless of the type of comonomers, the increase in the amount of comonomers lowers the encapsulation efficiencies of microcapsules. These phenomena are assumed to be due to the increasing hydrophilicity in the case of MAA and the decreasing hardness in the case of EMA and BMA.¹⁶ Through the combining the

chemical affinity of comonomers and latent heat capacity of microcapsules, it is estimated that comonomers that have chemical affinity to paraffins and able to form hard molecular chain network in the shell are effective to enhance the encapsulation efficiencies of microcapsules.

Thermal Stability. Thermogravimetric analyses (TGA) were performed to investigate the thermal stability of prepared microcapsules. In Figures 16 and 17 results of microcapsules prepared by using suspension and emulsion polymerization

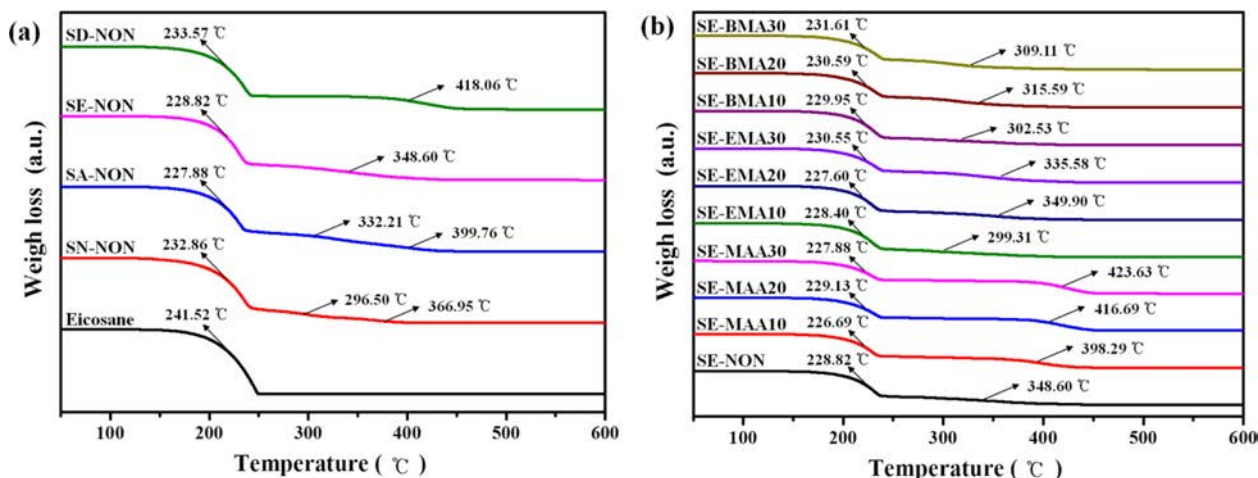


Figure 16. TGA thermograms of the microcapsules prepared by suspension polymerization with various crosslinking agents (a) and comonomers (b) differing in their weight portions.

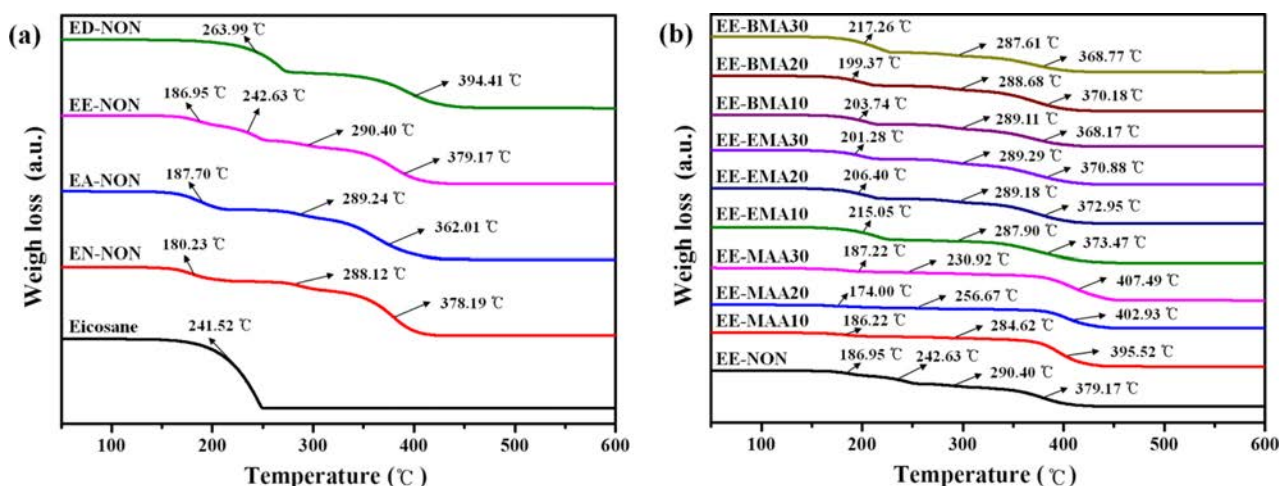


Figure 17. TGA thermograms of the microcapsules prepared by emulsion polymerization with various crosslinking agents (a) and comonomers (b) differing in their weight portions.

methods are summarized, respectively. It is found that the boiling point of eicosane and monomer MMA are 341 and 101 °C, respectively. All the TGA curves of microcapsules show two-step weight loss. The first weight losses, at around 200 °C, are related to the core PCM eicosane, because pure eicosane shows only one-step weight loss around this range. These first weight losses are assumed to be due to evaporation of eicosane in the form of pure or azeotropic mixture with other impurity such as water and residual monomers. Other weight losses that appear at higher temperature should be related to the polymeric shell; they show wide variation according to the shell components. The weight loss of encapsulating polymeric shell at a sufficiently higher temperature than PCM eicosane means that

PMMA has enough thermal stability for the application as a shell material encapsulating paraffins, irrespective of the selection of crosslinking agents and comonomers.

The shell of microcapsules prepared without crosslinking agents is observed to have low thermal stability, as shown in Figure 16(a) and Figure 17(a). Compact molecular chain networks formed through the input of crosslinking agents are assumed to raise the temperature of thermal degradation.¹³ This investigation is also supported by that the microcapsules containing DVB moiety of hard phenyl unit showing best thermal stability.

Through the input of comonomer MAA and increase of its quantity, it is possible to enhance strongly the thermal stability

of shell of microcapsules compared to PMMA homopolymer networks, as shown in Figure 16(b) and Figure 17(b). On the other hand, the input of comonomers such as EMA and BMA, which provide a softer molecular segment, lowers the thermal stability of polymeric shell networks than the PMMA homopolymer networks.¹⁶

The thermal stability of microcapsules prepared by emulsion polymerization was far inferior to the ones from suspension polymerization. The weight losses related to eicosane appear usually at temperature lower by around 30 °C than the cases of suspension polymerization. Second-step weight loss of microcapsule's shell prepared by emulsion polymerization begins slightly at around 280 °C, which is estimated as the decomposition of terminal double bond formed during polymerization reaction by the disproportionation termination, followed by decomposition accompanying chain scission around 360 °C.¹⁷

Conclusions

For the microencapsulation of paraffin PCMs with PMMA polymer system, the use of the suspension polymerization system is much better than emulsion polymerization for easy handling enhanced encapsulation efficiency of microcapsule particles. Crosslinking agents that supply compact and stiff connections between PMMA main chains are better for higher latent heats of core paraffin. In the selection of comonomers to adjust the mechanical properties of shell such as hardness and toughness, high hydrophilic comonomers are not proper for retention of high encapsulation efficiency, although they help the formation of smooth and hard shell surface through water affinity. The comonomers having the side chains compatible with chemical frame of paraffin should help to raise encapsulation efficiency of microcapsules. For the storage of higher latent heat in the core and higher thermal stability of shell, it is necessary to input crosslinking agents and comonomers that supply chemical affinity to paraffin as well as short and hydrophobic connections between PMMA main chains.

Acknowledgements: This work was supported by a research fund in 2016 from Chungnam National University.

References

1. C. Liu, Z. Rao, J. Zhao, Y. Huo, and Y. Li, *Nano Energy*, **13**, 814 (2015).
2. J. C. Kurnia, A. P. Sasmito, S. V. Jangam, and A. S. Mujumdar, *Appl. Therm. Eng.*, **50**, 896 (2013).
3. H. Zhang and X. Wang, *Sol. Energy Mater. Sol. Cells*, **93**, 1366 (2009).
4. J.-S. Cho, A. Kwon, and C. G. Cho, *Colloid Polym. Sci.*, **280**, 260 (2002).
5. P. Siddhan, M. Jassal, and A. K. Agrawal, *J. Appl. Polym. Sci.*, **106**, 786 (2007).
6. G. Fang, H. Li, F. Yang, X. Liu, and S. Wu, *Chem. Eng. J.*, **153**, 217 (2009).
7. Y.-H. Jo, Y.-K. Song, H.-C. Yu, S.-Y. Cho, S. V. Kumar, B.-C. Ryu, and C.-M. Chung, *Polym. Korea*, **35**, 152 (2011).
8. F. Salaün, E. Devaux, S. Bourbigot, and P. Rumeau, *Chem. Eng. J.*, **155**, 457 (2009).
9. Y. Jung, J. O. You, and K. H. Youm, *Macromol. Res.*, **23**, 1004 (2015).
10. A. Sari, C. Alkan, D. K. Döğüşcü, and A. Biçer, *Sol. Energy Mater. Sol. Cells*, **126**, 42 (2014).
11. L. Sánchez, P. Sánchez, A. de Lucas, M. Carmona, and J. F. Rodríguez, *Colloid Polym. Sci.*, **285**, 1377 (2007).
12. L. Sanchez-Silva, J. Tsavalas, D. Sundberg, P. Sánchez, and J. F. Rodríguez, *Ind. Eng. Chem. Res.*, **49**, 12204 (2010).
13. X. Qiu, W. Li, G. Song, X. Chu, and G. Tang, *Sol. Energy Mater. Sol. Cells*, **98**, 283 (2012).
14. A. Sari, C. Alkan, and C. Bilgin, *Appl. Energy*, **136**, 217 (2017).
15. H. Zhang and X. Wang, *Colloids Surf. A: Physicochem. Eng. Asp.*, **332**, 129 (2009).
16. X. Qiu, W. Li, G. Song, X. Chu, and G. Tang, *Energy*, **46**, 188 (2012).
17. A. Sari, C. Alkan, and A. Karaipekli, *Appl. Energy*, **87**, 1529 (2010).